



Representation of disturbance in the Joint UK Land Environment Simulator Vn4.8 (JULES)

Chantelle Burton^{1,2}, Richard Betts^{1,2}, Manoel Cardoso³, Ted R. Feldpausch², Anna Harper², Chris Jones¹, Douglas I. Kelley⁴, Eddy Robertson¹, Andy Wiltshire¹

5 ¹Met Office Hadley Centre, Exeter, UK. EX1 3PB, UK

²College of Life and Environmental Science, University of Exeter, Exeter. EX4 4SB. UK

³Brazilian Institute for Space Research (INPE), Earth System Science Center (CCST), São José dos Campos, Brazil

⁴Centre for Ecology and Hydrology, Wallingford. OX10 8BB. UK

10 *Correspondence to:* Chantelle Burton (chantelle.burton@metoffice.gov.uk)

Abstract

The representation of disturbance is a critical factor in land-surface modelling, but is generally poorly constrained in carbon cycle models. In particular, land-use change and fire can be treated as large-scale disturbances without full representation of their underlying complexities and interactions. Here we describe developments to the land surface model JULES (Joint UK Land Environment Simulator) to represent land-use change and fire as separate disturbances. We use the HYDE (History Database of the Global Environment) land cover dataset to analyse the impact of land-use change on global vegetation, and couple the fire model INFERNO (INteractive Fire and Emission algoRithm for Natural envirOnments) to dynamic vegetation within JULES to assess how the representation of disturbance affects the simulation of present day vegetation. We test model performance, evaluating the inclusion of land use and fire disturbance against standard benchmarks. Using the Manhattan Metric, overall disturbance improves the simulation of vegetation cover compared to observations by up to 53%. Grasses show an improvement of up to 52%, with biases in extent reduced from -66% to 13%. Total woody cover improves by up to 121% from a reduction in forest extent in the tropics, although simulated tree cover is now too sparse in some areas. Disturbance generally decreases tree and shrub cover and increases grasses. The results show that the disturbances provide important contributions to the realistic modelling of vegetation on a global scale, although in some areas fire and land-use together result in over-disturbance. This work provides a substantial contribution towards representing the full complexity and interactions between land-use change and fire that could be used in Earth System Models.

1 Introduction

Land-use change and fire are two of the most important disturbances that occur in the Earth system. These disturbances affect vegetation dynamics (e.g. Lasslop et al., 2016), atmospheric chemistry (Crutzen et al., 1979), the hydrological cycle (Shakesby



and Doerr, 2006) and the carbon cycle (Prentice et al., 2011), as well as surface albedo (López-Saldaña et al., 2015) and feedbacks on radiative forcing. Each year around 4% of vegetation is burned (Giglio et al., 2013), releasing approximately 2 PgC which equates to around a quarter of emissions from fossil fuel combustion (Hantson et al., 2016; van der Werf et al., 2017). Land-use and land-cover change (LULCC) can include clearance through fire, as well as other forms of deforestation, conversion of natural vegetation to agricultural land, and abandonment of agricultural land with subsequent forest regrowth. At least 50% of the ice-free land surface has been affected by land-use activities over the last 300 years; 25% of global forest area has been lost, and agriculture now accounts for around 30% of the land surface (Hurt et al., 2011). LULCC can result in changes to biogeochemical and biophysical properties of the Earth system, including changes to surface fluxes of radiation, aerodynamic roughness, heat and moisture, evaporation patterns, soil moisture and latent heat (Betts 2005).

The representation of disturbance, in particular fire, drought and tree mortality in models is poorly constrained, as identified in the most recent IPCC report (Ciais et al., 2013; Flato et al., 2013). This paper focuses on developments to the representation of LULCC and fire in the community land surface model JULES (Joint UK Land Environment Simulator). Previously in JULES, fire disturbance has not been represented as a separate process, but included in a generic large-scale disturbance term as a spatially-constant turnover rate. The purpose of this paper is to document the developments to the model to include the explicit representation of fire and land-use, and to evaluate the impact of these developments on the simulation of vegetation within JULES.

2 The interaction of fire and LULCC

LULCC is known to be one of the most important influencing factors in the decline of forests in several ways: directly through deforestation and canopy thinning (cutting as well as use of fire for clearance), and through fire-leakage which can extend forest losses into much larger areas than planned. Fragmentation is also an important contributing factor, causing increased tree mortality and carbon losses near the forest edges (Laurance et al., 2000), and increased spread of fire into the forest (Soares-Filho et al., 2006; Coe et al., 2013; Good et al., 2014). This can be the result of land clearance for agriculture, and for urban expansion. For example there is a clear correlation between distance to roads and increased fire risk in Amazonia (Cardoso et al., 2003). Even when deforestation itself declines, fire incidence can remain high due to increased agricultural frontiers where accidental fires burn out of control (Aragão and Shimabukuro 2010; Cano-Crespo et al., 2015) exacerbated by drought conditions (Aragão et al., 2018). Small-scale forest degradation is sometimes included in the definition of LULCC and can be an important contributor to carbon and biomass loss, however more frequently these contributions are below the level of detection and are often not accounted for in estimates of LULCC (Watson et al., 2000; Arneth et al., 2017). Similarly small fires are difficult to detect by conventional satellite methods (Randerson et al., 2012), leading to potential underestimations in LULCC and emission reporting.

The interaction between fire and managed agricultural land is complex. Small scale croplands are often burnt to clear land before planting or harvesting, and can also be burnt after harvest to dispose of waste, where pasture lands may be burnt to



fertilise the soils between crops (Rabin et al., 2017a). Agricultural land may therefore be an important contributing factor in fire emissions, and fire ignition. Conversely, larger agricultural lands may provide a fire break, where more active fire management takes place to prevent fires from spreading into crop areas unintentionally. Andela et al. (2017) has shown that fire occurrence has been reducing in many regions because of an increasing shift towards urbanisation and mechanised agriculture, making fuel less readily available and decreasing ignitions. These processes are difficult to represent in large scale models and are often not included explicitly in fire models.

Future fire activity will depend on a combination of both anthropogenic and climatic factors. Forest susceptibility to fire is projected to change little for low emissions scenarios, but substantially for high emissions scenarios (Settele et al., 2014; Burton et al., 2018). Because the frequency of fires increases with temperature, the IPCC AR5 report concluded that the incidence of fires is expected to rise over the 21st Century (Flato et al., 2013) although there is low agreement in the models on a regional scale due to the complexity of interactions and feedbacks and lack of proper representation in models (Settele et al., 2014). However while the meteorological conditions may become more conducive to fire risk in the future, the effects of future LULCC will also have a direct impact on how fire risk will change. LULCC can have important impacts on regional climate, and has been shown to reduce evapotranspiration (Cochrane and Laurance 2008), decrease precipitation and induce drought (Bagley et al., 2014), which can in turn initiate abrupt increases in fire-induced tree mortality (Brando et al., 2014; Castello and Macedo 2016). In order to model the impacts of these changes in the future, disturbance needs to be properly represented in Dynamic Global Vegetation Models (DGVMs).

The interaction of LULCC, climate change and fire is complex (Coe et al., 2013) and in order to understand the multiple positive feedbacks comprehensively, it is necessary to consider all of these elements together (Aragão et al., 2008). Here we begin to address some of these complexities, by developing a separate fire disturbance term within the land surface model JULES, and using interactive land-use, with the aim of ultimately being able to represent these processes within a fully coupled Earth System Model.

3 Model description and developments

JULES is a land surface model which simulates surface fluxes of water, energy and carbon, along with the state of terrestrial hydrology, vegetation and carbon stores (Clark et al., 2011; Best et al., 2011). Within JULES a DGVM called TRIFFID (Top-down Representation of Interactive Foliage and Flora Including Dynamics) is used to represent the carbon cycle and the distribution of different Plant Functional Types (PFTs) (Clark et al., 2011; Cox et al., 2000; Cox et al., 2001). Here we focus on the simulation of PFT distribution in a global model run, that is, the area of each grid box covered by PFT i : v_i .

$$\frac{dv_i}{dt} = \frac{\lambda \Pi v_*}{C_{vi}} \left\{ 1 - \sum_j c_{ij} v_j \right\} - \gamma_v v_*$$

30

(1)



Equation (1) is used to calculate the evolution of v_i . The rate of increase of v_i depends on the carbon available for increasing PFT area ($\lambda \Pi v_*$) and the carbon cost of increasing area, given by the carbon density (C_{vi}). Two terms balance the constant expansion of PFTs; a competition term (within the curly brackets) represents the loss of PFT area due to competition for limited space, and a disturbance term ($\gamma_v v_*$) representing vegetation loss due to all mortality processes not related to competition. λ is the fraction of NPP per PFT area, Π , used for increasing PFT area. v_* is the maximum of PFT area, v_i , and a minimum of 0.01 gridbox fractional area, imposed to ensure PFTs do not get permanently removed from a given gridbox. c_{ij} determines which of PFTs i or j is dominant and will out compete the other. The configuration used here has 5 PFTs; the 2 tree PFTs out-compete the shrub PFT, the shrub PFT out-competes the 2 grass PFTs, and the taller of the 2 tree /grass PFTs out-competes the shorter tree /grass PFT. γ_v is a PFT-dependent disturbance rate.

10

The effect of land-use on vegetation distribution is included by modifying the competition term of Eq. (1). In the competition term, c_{ij} is zero for dominant PFTs, meaning the whole gridbox is available for PFT i to expand into. For non-dominant PFTs, c_{ij} is 1 and expansion is scaled by the fraction of the gridbox where PFT i is dominant. Land-use is also represented by a limitation to the space available for a PFT to expand into. A fraction of each gridbox is prescribed as the “disturbed fraction”, which represents the area covered by agriculture, with no distinction between cropland and pasture being made. When land-use is added to Eq. (1), we have:

15

$$\frac{dv_i}{dt} = \frac{\lambda \Pi v_*}{C_{vi}} \left\{ 1 - \alpha a_i - \sum_j c_{ij} v_j \right\} - \gamma_v v_* \quad (2)$$

Where α is the disturbed fraction and a_i is 1 for non-woody PFTs and 0 for woody PFTs. The three woody PFTs (broadleaf trees, needle-leaf trees and shrubs) are prevented from growing in the disturbed fraction, while the two grass PFTs (C3 grass and C4 grass) can grow anywhere in the gridbox. Grass PFTs growing in the disturbed fraction are interpreted as agricultural grasses, although they are physiologically identical to “natural” grasses. α can increase or decrease over time. As α increases, first “natural” grasses are relabelled as “agricultural” grasses, then an area of woody PFTs is replaced by bare soil, which can be replaced by the non-woody PFTs over time if they are viable. As α decreases, an area of “agricultural” grasses is relabelled as “natural” and becomes available for woody PFTs to expand into.

25

PFT	Broadleaf Tree	Needle-leaf Tree	Shrub	C3 Grass	C4 Grass
γ_v implicit fire	0.009	0.0036	0.05	0.10	0.10
γ_v using INFERNO	0.0045	0.0018	0.15	0.10	0.10

Table 1: The disturbance rate, γ_v , implicitly including fire disturbance (top row) and excluding fire disturbance (bottom row).



The effect of fire on vegetation distribution is included by modifying the disturbance rate, γ_v . Previously disturbance due to fire was implicitly included in γ_v , along with mortality due to pests, windfall and many other processes. Fire disturbance, β_i , is included as a PFT-dependent burnt area which can vary in space and time. β_i is calculated within JULES by the INFERNO (INteractive Fire and Emission algoRithm for Natural enviroNments) fire model (Mangeon et al., 2016). Now that fire is explicitly represented, γ_v must be reduced accordingly, hence the representation of fire does not necessarily increase mortality, but makes it spatially and temporally variable. Table 1 shows the values of γ_v ; in the top row values implicitly include fire disturbance before the coupling, and in the bottom row fire is treated separately using INFERNO. Equation 3, includes fire along with land-use:

$$\frac{dv_i}{dt} = \frac{\lambda \Pi v_*}{C_{vi}} \left\{ 1 - \alpha a_i - \sum_j c_{ij} v_j \right\} - (\gamma_v + \beta_i) v_*$$

10 (3)

The calculation of burnt area depends on fuel availability including soil carbon density, C_s , providing additional mechanisms by which fire and land-use can feedback onto vegetation distribution. The coupling of fire and the carbon cycle includes a direct impact of fire on C_s ; some soil carbon is burnt, resulting in a flux of carbon from the soil to the atmosphere. The burnt soil carbon flux is diagnosed in INFERNO and we now allow the flux to effect the evolution of C_s . The carbon cycle in JULES does not explicitly represent a litter carbon store, however the model includes four soil carbon pools and we use two of these pools as proxies for flammable litter. The decomposable plant material soil carbon pool, C_{dpm} , and the resistant plant material soil carbon pool, C_{rpm} , both receive the litter carbon flux from vegetation and have a relatively rapid turnover rates, making them reasonable proxies for the litter carbon store. The calculation of the burnt soil flux is similar to INFERNO's diagnosis of the burnt vegetation flux (equation 8 of Mangeon et al., 2016).

$$20 \quad f_s = \left(\mu_{min,k} + (\mu_{max,k} - \mu_{min,k})(1 - \theta) \right) C_k \sum_i \beta_i v_i$$

(4)

The efficiency of soil burning is inversely proportional to the surface soil moisture, θ , with the values of the completeness of combustion parameters, μ , for each soil pool, k , being listed in Table 2. The burnt soil flux is proportional to the total available fuel, C_k , and the total burnt area, summed over all PFTs.

25

Soil Carbon Pool	Decomposable plant material, C_{dpm}	Resistant plant material, C_{rpm}
μ_{min}	0.8	0.0
μ_{max}	1.0	0.2

Table 2: Completeness of combustion parameters.



Fire and land-use both affect the soil carbon store by altering the vegetation-to-soil litter flux. Without fire or land-use, the litter flux comprises a local litter fall rate, Λ_l , representing the turnover of leaves, roots and stems, litter due to disturbances and litter due to competition. The total litter fall is defined by Clark et al. (2011) as (their equation 63):

$$\Lambda_c = \sum_i v_i \left(\Lambda_{li} + \gamma_{vi} C_{vi} + \Pi_i \sum_j c_{ij} v_j \right) \quad (5)$$

Including our new disturbance terms produces:

$$\Lambda_{CvLoss} = \sum_i v_i \left(\Lambda_{li} + (\gamma_{vi} + \beta_i) C_{vi} + \Pi_i \sum_j (\alpha a_i + c_{ij} v_j) \right) \quad (6)$$

- 10 The new term, Λ_{CvLoss} , still represents a loss of vegetation carbon, but now not all of this flux enters the soil carbon pools, instead some of the vegetation carbon loss due to fire is lost to the atmosphere and some of the loss due to land-use change enters wood product carbon pools. All litter fluxes that do enter soil carbon pools are split between C_{dpm} and C_{rpm} according to PFT-specific parameters as described by Clark et al. (2011). To calculate the losses due to the new processes the vegetation distribution (Eq. 3) and vegetation loss (Eq. 6) are calculated with and without the new process, and the difference between
- 15 the two values of Λ_{CvLoss} is attributed to the new process.

The litter due to land-use change, Λ_{LUC} , is calculated by repeating Eq. (3) and (6) with the disturbed fraction from the previous timestep, α_{-1} ; note that both calculations include some disturbed fraction and it is the litter due to land-use *change* that is being calculated, not the effect of existing land-use.

$$\Lambda_{LUC} = \Lambda_{CvLoss} - \sum_i v_{LUC,i} \left(\Lambda_{li} + (\gamma_{vi} + \beta_i) C_{vi} + \Pi_i \sum_j ((\alpha - \alpha_{-1}) a_i + c_{ij} v_{LUC,j}) \right) \quad (7)$$

Where, v_{LUC} , is the PFT area calculated by Eq. (3) with $\alpha = \alpha_{-1}$. Λ_{LUC} is distributed between the soil carbon pools and the wood product pools; the portion that is below ground carbon, given by (root carbon/ C_v), is added to the soil carbon pools and the remaining above ground portion is added to the wood product pools (Jones et al., 2011).

- 25 Carbon loss due to fire, Λ_{Fire} , is calculated by repeating Eq. (3) and (6) with no burnt area ($\beta=0$):

$$\Lambda_{Fire} = \Lambda_{CvLoss} - \sum_i v_{NoFire,i} \left(\Lambda_{li} + \gamma_{vi} C_{vi} + \Pi_i \sum_j (\alpha a_i + c_{ij} v_{NoFire,j}) \right) \quad (8)$$



Where v_{NoFire} , is the PFT area calculated using Eq. (3) with $\beta=0.13$, meaning that 13% of the vegetation carbon killed by fire is emitted and the remainder enters the soil carbon pools (Li et al., 2012).

4 Methods

Here we run JULES Vn4.9 with CRU-NCEP7 forcing data for climate and CO₂, and land-use ancillaries from HYDE (History Database of the Global Environment) (Le Quéré et al., 2016) from 1860 to present day. The harmonised HYDE dataset estimates fractional land-use patterns and underlying transitions in land-use annually for 1500-2100, and is spatially gridded at half degree resolution. It does not include impacts of degradation, climate variability, forest management, fire management or pollution on land cover (Hurt et al., 2006). This was then re-gridded for use in JULES at N96 resolution (1.25° latitude x 1.875° longitude).

For the fire experiments, the model was spun-up for 1000 years with fire on using pre-industrial land-use and CO₂ at 1860 prescribed as a climatology. INFERNO was run here with constant natural and anthropogenic ignitions, and interactive fire-vegetation on.

The model was tuned with fire towards a PFT distribution from the European Space Agency Climate Change Initiative (ESA CCI, 2010) observations, using maximum spreading (λ) as LAI_{min}= 1.0, and the large-scale disturbance term (γ_v) modified as per Table 1. Altering LAI_{min} is a way of increasing the rate of spread of vegetation to account for a known deficiency in the model associated with slow regrowth. The large-scale disturbance of trees has been halved and disturbance of shrub increased by a factor of three to be within the error bars of ESA observations.

JULES was configured to the TRENDY set up (Sitch et al., 2015) using two experiments: S2 = CO₂ and climate forcing (with land-use constant at 1860, referred to as ‘No LULCC’); and S3 = CO₂, climate and land-use forcing, initially not including fire for the purposes of comparison. These two experiment configurations were repeated including fire (SF2 and SF3).

For benchmarking the performance of our model configurations, we use the protocol used by FireMIP (Rabin et al., 2017b) based on the benchmarking system outlined in Kelley et al. (2013). Annual average burnt area was assessed using the Normalised Mean Error (NME) metric, which sums the difference between the model (mod) and observations (obs) over all cells (i) weighted by cell area (A_i) and normalised by the average distance from the mean of observations \overline{obs} :

$$NME = \frac{\sum A_i \cdot |mod_i - obs_i|}{\sum A_i \cdot |obs_i - \overline{obs}|} \quad (9)$$

NME comparisons are conducted in three steps. Step 1 compares simulated and observed annual average burnt area. For step 2, mod_i and obs_i become the difference between modelled or observed and their respective area weighted means, i.e. $x_i \rightarrow x_i - \bar{x}$, thereby removing systematic bias to describe the performance of the model about the mean. Step 3 additionally removes the mean deviation i.e. $x_i \rightarrow x_i / |\bar{x}_i|$ and describes the models ability to reproduce the spatial pattern in burnt area.



Comparisons are made against fire CCI (Alonso-Canas and Chuvieco, 2015), MCD45 (Archibald et al., 2013), GFED4 (Giglio et al., 2013), GFED4s (van der Werf et al., 2017).

Simulated vegetation fractions are compared against Vegetation Continuous Fields (VCF) from MODIS (2002-2012), as recommended for fireMIP analysis (Rabin et al., 2017b), and ESA CCI reference observations, using the Manhattan Metric

5 (MM):

$$MM = \sum_{ij} A_i \cdot |mod_{ij} - obs_{ij}| / \sum_i A_i \quad (10)$$

Where j is vegetation type. Using the MM, we assess model performance against different vegetation combinations (see table SI-3 for a full list of comparisons).

10 All benchmark datasets were resampled from their native resolutions to N96 before comparison. Scores for all metrics are directly comparable across models, e.g. a score of 0.6 is twice as close to observations as 1.2, which we describe as 100% improvement from the control as per Kelley et al. (2014). Three null models are used for further interpretation (Table SI-4). The median and mean null model scores compare the median or mean of all observations with the observation data. Randomly-resampled null models compare resampled observations (without replacement) against observations, using 1000 bootstraps to

15 describe the distribution of the null model. Individual model quality can be described in terms of number of null models exceeded (Table 3).

5 Results

Here we present results showing the effect of LULCC and fire on the simulation of vegetation in JULES. First, we present global vegetation by PFT to assess the present day spatial distribution of vegetation as a result of LULCC disturbance compared

20 to observations. We then move on to fire disturbance, first reviewing how the new fire disturbance term modelled by the coupled INFERNO model compares to GFED observations of burnt area as validation for the fire model. We then present global vegetation by PFT for fire disturbance and show how this compares to observations. Finally we show the global distribution of vegetation in the context of observations considering uncertainty bounds.

25 Without explicit fire or LULCC disturbance, the model produces too much broadleaf vegetation compared to observations, especially over South America and SE Asia (Fig. 1, second column). Both broadleaf and needleleaf trees are not simulated well in the high latitude boreal regions in JULES, and do not extend far enough across this region, which is not improved by adding disturbance. Overall the model performs poorly at simulating tree cover, as indicated by a MM score of 0.78 for vegetation cover comparison and 0.64 for wood cover (Table 3) when comparing against VCF (generally worse than our null

30 models – Table SI-4), and 0.72 and 0.45 respectively compared to CCI. The introduction of LULCC generally results in a reduction in broadleaf, needleleaf and shrub vegetation, and an increase in C3 and C4 grasses (Fig.1, fourth column), improving



the simulation of vegetation cover by up to 30% (20% against CCI, Table 3). This is as expected, with the purpose of this disturbance term being to represent crop area with C3 and C4 grasses. With LULCC, the broadleaf fraction is much improved over South America compared to observations, but is not improved in the high latitude regions. C3 grass is improved with LULCC, but the fraction is still too low, whereas shrub fraction remains too high (also shown in Fig. 5). The bare soil fraction is too high in the model, but the inclusion of LULCC has little effect on this.

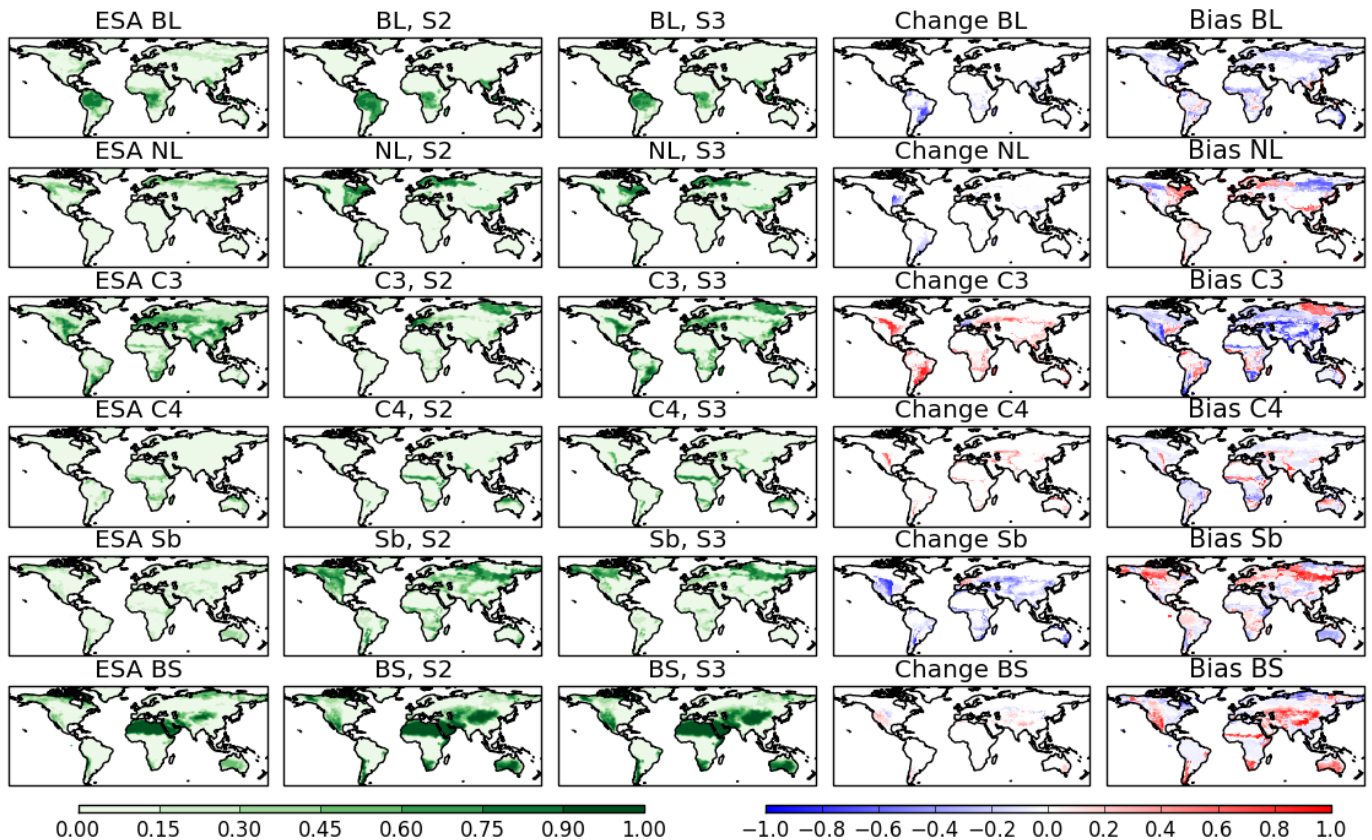


Figure 1: Present day (2015) vegetation fractions for the TRENDY S2 (without LULCC) and S3 experiment (with LULCC) by PFT, without fire, compared to observations. Left column shows ESA CCI observations (2010), second column shows vegetation without LULCC (S2), third column shows vegetation with LULCC (S3), fourth column shows the change resulting from LULCC (difference between column 2 and 3), and right column shows bias of S3 compared to observations (difference between column 1 and 3). BL = broadleaf, NL = needleleaf, C3 = C3 grasses, C4 = C4 grasses, Sb = shrub, BS = bare soil.

Now considering fire, compared to observations of burnt area from GFED 4.1s (including small fires) INFERNO captures the spatial extent and level of fire relatively well (Fig. 2 and Table SI-4). INFERNO accurately simulates the areas of high fire occurrence found in GFED4.1s, especially over Africa, northern Australia, South America and SE Asia, although the model also shows high fire occurrence over India which is not seen in the observations. This is likely due the current lack of representation of fire suppression in agricultural and urbanised areas. An NME score of 0.79-0.95 (Table SI-4) outperforms



all but one null model, and is better than published assessments of other global fire-vegetation models using the same metrics (Lasslop et al., 2014; Kelley et al., 2013; Kloster & Lasslop 2017; Hantson et al., 2016). NME step 2 and step 3 scores also fall in a similar range (Table SI-4) demonstrating a strong performance in overall fire magnitude, variance and spatial pattern.

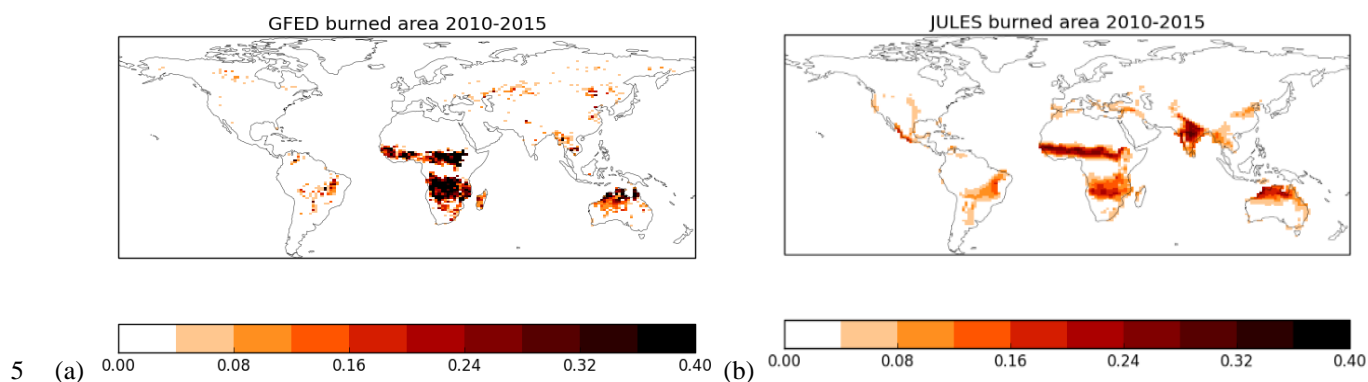


Figure 2: Average 2010-2015 burned area from GFED 4.1s observations (a) and as modelled by JULES-INFERN0 (b)

Similarly to LULCC, fire disturbance also improves the representation of vegetation cover, this time by around 44% compared to VFC (12.5% against CCI, Table 3). The balance of tree to grass cover over South America for example shows particular improvement (Fig. 3, third column), although in other areas fire creates too much disturbance and results in tree fraction being too sparse, notably across Africa (although still within the range of uncertainty, see Fig. 4). C3 grass fractions are generally too low without fire compared to observations, and this is improved with fire. C4 grasses are well modelled both with and without fire (Table 3). The shrub fraction is too high in the model compared to observations, but this is also improved when fire is included (38%, Table SI-4, and also shown in Fig. 5). There is too much bare soil in the model without disturbance, and this increases further with fire. The overall change as a result of fire is generally a reduction in the larger PFTs (broadleaf and needleleaf trees) and an increase in grasses and bare soil (Fig. 3, fourth column). Broadleaf trees show a loss in all regions, including the Cerrado region to the south of the Amazon, across the arid regions in Africa, SE Asia, and northern high latitudes. The changes in shrub and C4 grasses are more variable, and are region-dependent. The increase in grasses and bare soil reflects the burnt area as modelled by INFERN0 (Fig. 2b), indicating shift away from woody vegetation (broadleaf trees, needleleaf trees and shrubs) towards faster growing vegetation and bare ground as a result of fire.

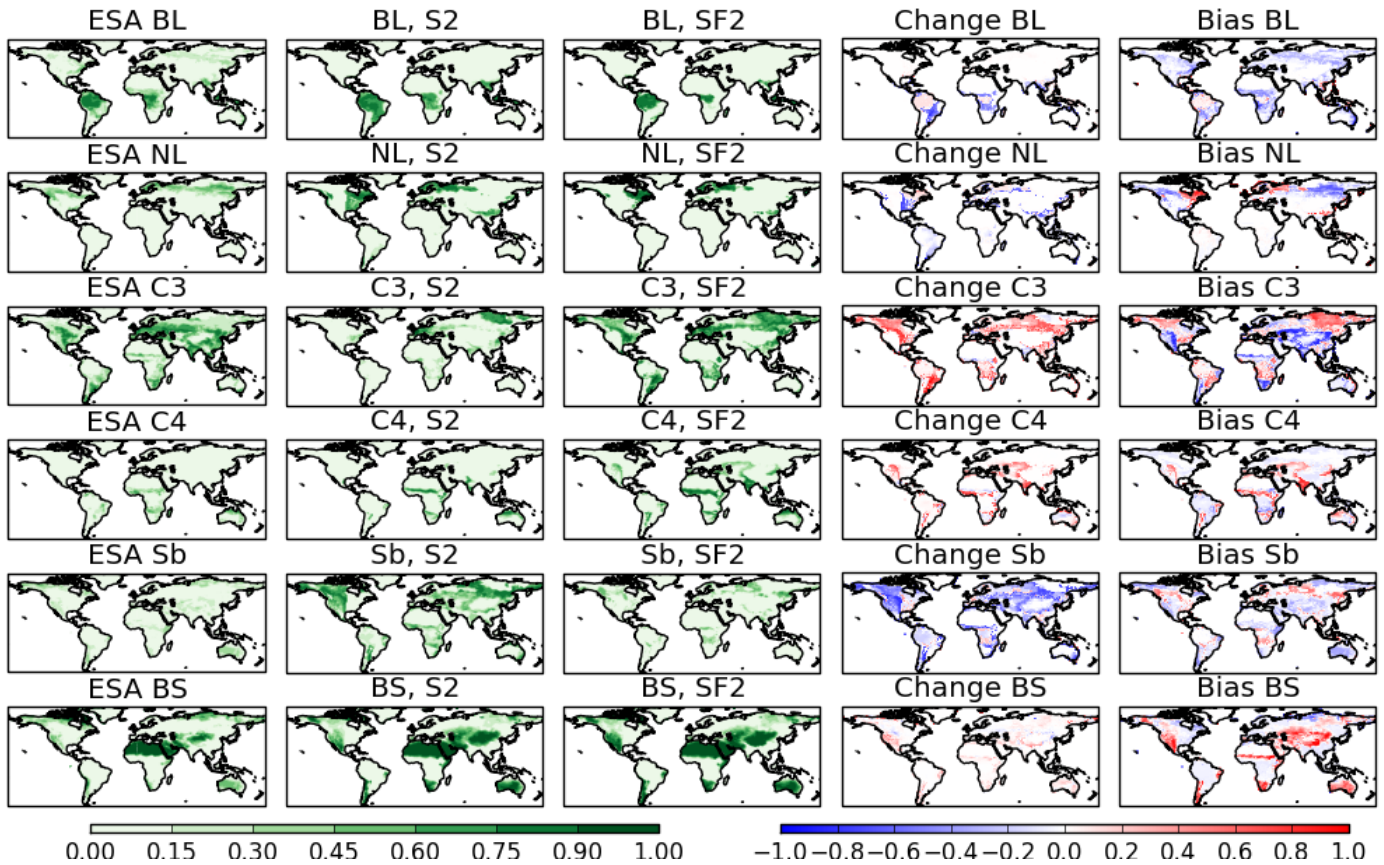


Figure 3: Present day (2015) vegetation fractions for the TRENDY S2 experiment (no LULCC, no fire) and SF2 (fire only) by PFT compared to observations. Left column shows ESA CCI observations (2010), second column shows vegetation without fire or LULCC (S2), third column shows vegetation with fire only (SF2), fourth column shows the change resulting from fire (difference between column 2 and 3), and right column shows the bias of SF2 compared to observations (difference between column 1 and 3). BL = broadleaf, NL = needleleaf, C3 = C3 grasses, C4 = C4 grasses, Sb = shrub, BS = bare soil.

5

As with all observational datasets, there are uncertainties associated with retrieving observations of land cover and the classification of these into a small number of plant functional types. The observations used here are from ESA CCI, which have been processed into the 5 PFTs used by JULES so as to be comparable with the model output (Hartley et al., 2017), introducing a range of possible values for each vegetation type. The representation of vegetation distribution is further complicated by the seasonal variation, where peak growing season will have higher fraction of vegetation than low season, and high fire-risk areas will show burnt area as high bare soil in peak fire season. These uncertainties give a range of potential vegetation cover, and the developments to the representation of disturbance in JULES described here have been tuned to give reasonable distribution within this range of uncertainty as far as possible (Fig. 4 and Fig. 5 top left panel). The ‘best estimate’ of vegetation cover from ESA, known as the reference case, is otherwise used for comparison, and VCF used to provide additional comparison in the benchmarking assessment.

15

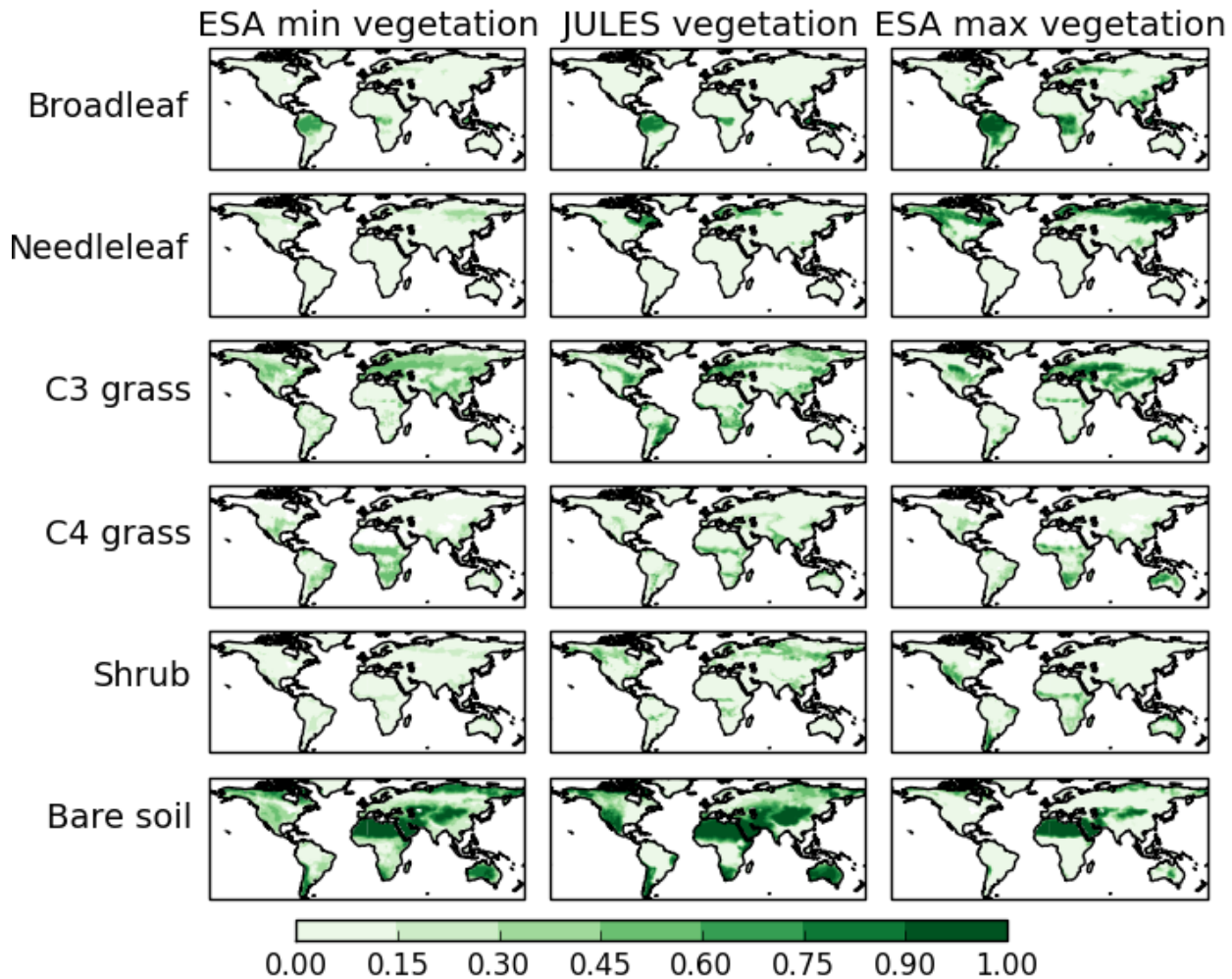


Figure 4: Present day (2015) vegetation fraction PFT, as modelled by JULES-INFERNO with LULCC (central column), compared to the range of uncertainty from ESA CCI observations (V1, 2010) (Minimum fractions left column, maximum fractions right column). Top row = broadleaf, second row = needleleaf, third row = C3 grass, fourth row = C4 grass, fifth row = shrub, sixth row = bare soil.

5

Considering the distribution by vegetation type (trees, grasses, shrubs and soil), in all cases adding disturbance to the model brings the global total vegetation closer to reference observations, although bare soil increases in the opposite trend (Fig. 5, top left panel). In the case of trees and shrubs, fire plus LULCC creates too much disturbance (42% and 47% less coverage than observations respectively), but grasses increase (13% more coverage than observations) (Table SI-1). This is reflected in only slight improvements in MM scores for vegetation cover and wood cover comparisons against VCF, and a slight degradation when compared against CCI (Table 3). Trees are reduced by 43% when both disturbances are included (S2 no fire compared to S3 with fire), shrubs by 71%, and grasses increase by 127% (Table SI-1), taking into account the updated terms

10

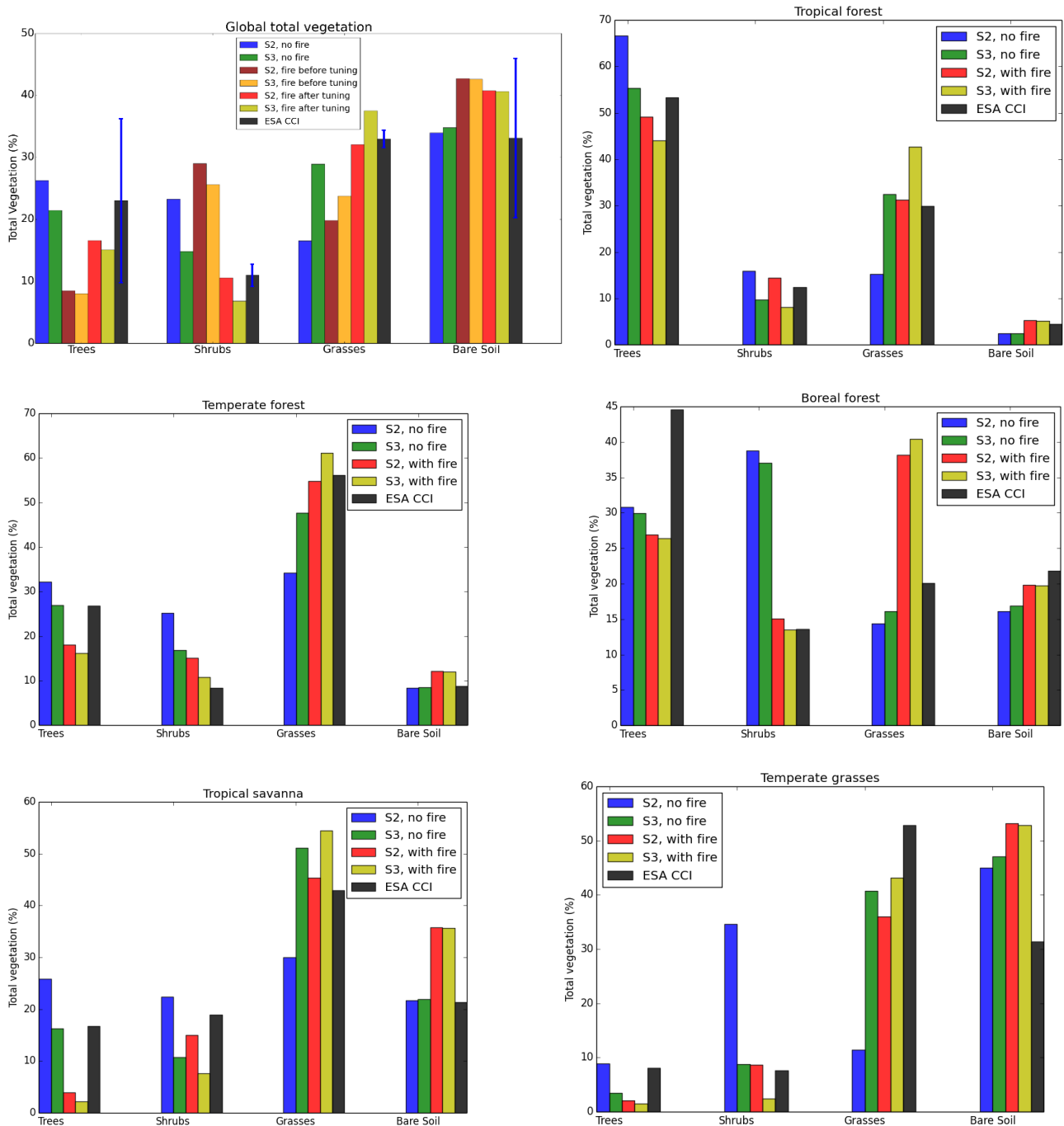


for γ_v (Table 1). There is an increase of 20% in bare soil with disturbance included. Overall, adding disturbance into JULES reduces the bias of shrubs from 72% to 47%, and grasses from -66% to 13% compared to observations (Table SI-1).

However there is more variation by biome. In all cases tree fraction is simulated as too low with both fire and LULCC although the extent of this varies. In some cases shrubs improve (in the temperate and boreal forests), but in others the results show too much disturbance (tropics, savanna and temperate grasses). Grasses are generally higher than observations, except for the temperate grasses biome. Both disturbance terms reduce the tree and shrub fractions, and increase grasses and bare soil fractions. In most biomes bare soil fraction is too high compared to observations, except in the tropics and boreal regions where the fraction is well represented compared to observations.

Overall, the inclusion of these disturbance terms within JULES leads to a shift towards grass cover and a reduction woody PFTs. This is as expected for land use, which replaces trees with grasses as a representation of crops. The regrowth rates for trees is much slower than for grasses, which spread fast and recover quickly (see section 3), which may be an important factor in the response to fire. With continuous disturbance which varies spatially and temporally now included in the model, the vegetation seems unable to recover trees in some areas, notably around the Cerrado and Congo regions, instead encouraging the growth of grasses in their place.

15



5 **Figure 5: Present day (2015) total vegetation (percentage) globally (top left), and by WWF biome (5 out of 8 shown here: tropical forest, temperate forest, boreal forest, tropical savanna, and temperate grasses. Tundra, Mediterranean wood and desert not shown). Trees = total broadleaf and needleleaf trees, grasses = total C3 and C4 grasses. Top left panel includes results prior to tuning, plus uncertainty bars for the observations shown in blue.**



Comparison	Observations	JULES				Improvement from control		
		S2: Control	S3: Land use only	SF2: fire only	SF3: Land use and fire	S3	SF2	SF3
Vegetation cover	VCF	0.78	0.60	0.54	0.51	30.00%	44.44%	52.94%
	CCI	0.72	0.60	0.64	0.63	20.00%	12.50%	14.29%
Tree Cover	CCI	0.35	0.28	0.30	0.30	25.00%	16.67%	16.67%
Wood Cover	VCF	0.64	0.43	0.33	0.29	48.84%	93.94%	120.69%
	CCI	0.45	0.31	0.35	0.36	45.16%	28.57%	25.00%
Grass Cover	VCF	0.64	0.48	0.43	0.42	33.33%	48.84%	52.38%
	CCI	0.43	0.33	0.40	0.42	30.30%	7.50%	2.38%

Table 3: Benchmarking results for each experiment by vegetation type, using VCF and CCI reference observations. Vegetation cover = woody, grass and bare soil cover for VCF and tree, shrub, grass and bare soil cover for cci. Woody cover = trees and shrubs vs other cover. Trees = BL and NL vs other cover. Grass cover = grass vs non-grass cover. Lower results for JULES = closer to observations. Colours indicate how many null models the configuration exceeds: Blue = all; green = all but one; yellow = only exceeds one; red = none exceeded.

10 6 Discussion

Fire and land-use are important global disturbances, and the results presented here have shown that when considered, they have a significant impact on the modelled vegetation as represented by JULES. In all cases, including disturbance brings the vegetation fractions closer to the observations compared to no disturbance, although in some cases there is a tendency towards over-disturbance when both fire and LULCC are included, and bare soil increases too much compared to observations (Fig. 5). Disturbance generally improves the simulation of shrubs and grasses, but tree fractions are often simulated as too sparse. LULCC mainly decreases trees and shrubs and replaces them with C3 and C4 grasses (representing crop and pasture). Fire creates a more mixed response, decreasing vegetation in the boreal regions and high fire risk areas, and showing an increase in grasses. Both fire and LULCC reduce the larger vegetation types when added to the model (Fig. 1 and 3). Without the inclusion of fire, this could result in an over-estimation in the amount of carbon released due solely to LULCC, which may have significant impact on carbon budgets.

Previous work has shown that fire may be an important contributor to the existence of savannas (Cardoso et al., 2008; Staver et al., 2011). The results shown here seem to support this conclusion, showing that when fire is included in the model there is a shift towards open savanna-like states in areas that climatologically could support trees without the incidence of fire,



including the Cerrado area of South Brazil, and savanna areas in Africa. Here we have shown that a large savanna region in South America is completely forested in the model without the addition of fire or anthropogenic LULCC.

Here we have used the ESA CCI land cover product as our observational data for comparison with the model output. The CCI product has been translated into the 5 PFTs that are used in JULES (Poulter et al., 2015), and through the process of data collection and classification, a number of uncertainties are introduced which result in a range of possible outcomes for land cover distribution (Hartley et al., 2017). These uncertainties can include variation in classifying the surface reflectance products into the 22 land cover classes, and aggregating these by dominant vegetation type into just 5 PFTs for JULES using a consultative cross-walking technique. This classification also take into account seasonal variation in NDVI (greenness), burned area, cloud cover and snow occurrence that can all vary throughout the year, giving a large range between the minimum and maximum possible vegetation cover for any one PFT, as shown in Fig. 4. For this reason we also use the MODIS VCF for benchmarking comparison. The VCF product is a characterisation of the land surface into just three components of ground cover using satellite data: tree cover, non-tree vegetation cover, and bare ground. The model performs well compared to a simple classification of tree and non-tree vegetation cover, showing the spatial coverage of vegetation is simulated well when both disturbances are added to JULES. The benchmarking results compared to CCI still show an improvement compared to the control, but on a global scale this is better when each disturbance is considered separately, suggesting further parameterisation may be beneficial for each PFT. However, it is important to consider regional improvements or degradation as well which can be masked in global scale analyses (Figs. 1,3,5). It also suggests that there may be some overlap in the disturbances, which reflects the complicated nature of how fire and LULCC are often used together for land clearance. The HYDE LULCC dataset in this study has been developed from a combination of model, satellite and historical reconstructions of agricultural and population data, and the biomass quantities are noted to contain uncertainties due to lack of direct observations from the historical period (Hurtt et al., 2011). Some of what has been attributed to LULCC may include fire clearance, which is a key point for consideration for other DGVMs including fire and land use together.

When interactive fire was initially added to JULES, there was a tendency towards complete dominance by shrubs and significant tree reduction (see Fig. 5, top left panel). This was tuned to the observations by increasing the large-scale disturbance term (γ) and increasing spreading (λ) (Table 1), to account for the fact that fire was previously included in the total mortality rate. Grasses spread and recover quickly with TRIFFID, whereas larger PFTs take longer to re-establish. On this timescale the tree cover is not able to recover fast enough with constant disturbance from fire, and the results indicate that fire restricts tree growth and encourages a shift towards the more responsive vegetation types. Grasses can be given a higher mortality rate to prevent over-growth, but this has been tested and results in too much bare soil for this reason. The fractions were low from the start of the run (1860) as fire was included in the spin-up, and the vegetation does not recover through the transient simulation due to continual disturbance, leading to present day levels being low. This perhaps points to a need for faster regrowth of trees within TRIFFID to cope with disturbance, for example by representing age or mass classes within each PFT to enable a range of successional stages to be represented. It is also worth noting that the fire disturbance is high in some areas in the model compared to observations (Fig. 2), which may lead to too much disturbance in these regions. In addition,



there remains significant underlying complexity around the interaction of LULCC and fire as discussed in section 2. For example, agricultural land in some regions may be a cause of fire ignition, whereas in other areas may act as a fire break or generate anthropogenic fire suppression. One way forwards for this could be to identify the average field size based on surrounding vegetation, and mask fire in larger agricultural regions, but allow smaller fields to include the probability of burning. There will also be additional complexity around the PFTs themselves where some species will be more fire resilient than other species, for example vegetation in high fire-risk areas often develops thicker bark for protection from fire, whereas other species may adapt to the fire and use it as a method of reproduction (Pellegrini et al., 2017). The representation of just five PFTs is a considerable simplification of the real world. Finally, we have just considered two of the main disturbances here. We have not considered windthrow, pests, and diseases etc., which for now are still aggregated into the generic large-scale disturbance term in JULES.

There are still a number of regions that require improvement in the simulation of vegetation. In all of the JULES simulations there are too few needleleaf trees across the boreal regions compared to observations. With fire, notably the trees across the extratropics and savanna regions such as the Congo region in Africa is reduced. Further work could be to develop these configurations into the 9 PFT set up by (Harper et al., 2016). In particular, recent work has shown that the distinction between evergreen and deciduous needleleaf trees has led to an improved representation of boreal forests within JULES which could improve these simulations (Harper et al., 2018).

7 Conclusion

This work has described the first steps in developing the land surface model JULES to represent fire and land-use as separate disturbances. The results have shown the significant contributions of these disturbances to changes in vegetation on a global scale. Without disturbance JULES simulates too much vegetation in most PFTs compared to observations, which is generally improved with the addition of fire and LULCC, although there is still regional variation. Disturbance generally has the effect of decreasing tree cover (43%) and shrubs (71%) and increasing grasses (127%). In places the disturbance is too high with both fire and LULCC and leads to vegetation being reduced too much. The regrowth rates in TRIFFID also mean that with constant disturbance from fire, there is a shift towards faster growing PFTs that can recover and spread quickly. Overall, representing disturbance in JULES improves the simulation of vegetation by up to 53%, with woody vegetation improving by up to 121% and grasses by up to 52%. The simulation of shrubs and grasses is much improved, with the bias reducing from 72% to 47%, and from 66% to 13% respectively. It is expected that fire risk will increase in the future with climate change as a result of hotter, drier conditions, but fire occurrence depends heavily on the interaction with LULCC. The developments to the model that have been outlined in this paper now give the capability to model future interactions between fire and LULCC and the impact that this could have on future vegetation density, spread and carbon storage. Overall we have presented results for an improved representation of mechanistic processes of disturbance in JULES using a non-optimised approach, with positive results to vegetation cover. This is a significant first step in the representation of highly complex factors surrounding



anthropogenic and natural disturbances in the model, and lays the foundation for future developments into Earth System models.

Code Availability

The JULES code used in these experiments is freely available on the JULES trunk from version 4.8 (revision 6925) onwards.

- 5 The rose suite used for these experiments is u-ap845, at Vn5.0 r9986. Both the suite and the JULES code are available on the JULES FCM repository: <https://code.metoffice.gov.uk/trac/jules> (registration required).

Acknowledgements

This work and its contributors (CB, RB, CJ, ER, AW) were supported by the Newton Fund through the Met Office Climate Science for Service Partnership Brazil (CSSP Brazil).

- 10 MC acknowledges support from the Brazilian BNDES/Amazon Fund Project MSA/BNDES/BIOMASSA-SUB 7.

The contribution by DK was supported by the UK Natural Environment Research Council through The UK Earth System Modelling Project (UKESM, Grant No. NE/N017951/1)

We would like to thank Nicolas Viovy and Philippe Ciais for making available their CRU-NCEP forcing data, and for their kind permission for its use in these model runs.

15 Author Contribution

CB updated the code in the JULES trunk to include fire mortality, with help and advice from ER, AW, RB, CJ, AH. CB drafted the text and made the figures. ER and CB co-wrote section 3 and the equations. DK performed the benchmarking. All authors have contributed to the analysis methods and to the text.

References

- 20 Alonso-Canas, I. and Chuvieco, E.: Global burned area mapping from ENVISAT-MERIS and MODIS active fire data, *Remote Sens. Environ.*, 163, 140–152, doi:10.1016/j.rse.2015.03.011, 2015.
- Andela, N., D. Morton, L. Giglio, Y. Chen, G. van der Werf, P. Kasibhatla, R. DeFries, G. Collatz, S. Hantson, S. Kloster, D. Bachelet, M. Forrest, G. Lasslop, F. Li, S. Mangeon, J. Melton, C. Yue & J. Randerson: A human-driven decline in global burned area, *Science*, 356, 1356-1361, 2017.
- 25 Aragão, L., Malhi, Y., Barbier, N., Lima, A., Shimabukuro, Y., Anderson, L., & Saatchi, S.: Interactions between rainfall, deforestation and fires during recent years in the Brazilian Amazonia, *Philosophical Transactions of the Royal Society B-Biological Sciences*, 363, 1779-1785, 2008.



- Aragão, L. & Shimabukuro, Y.: The Incidence of Fire in Amazonian Forests with Implications for REDD, *Science*, 328, 1275-1278, 2010.
- Aragão, L. and Co-authors: 21st Century drought-related fires counteract the decline of Amazon deforestation carbon emissions, *Nature Communications* 9, 536. doi:10.1038/s41467-017-02771-y, 2018.
- 5 Archibald, S., Lehmann, C. E. R., Gomez-Dans, J. L., and Bradstock, R. A.: Defining pyromes and global syndromes of fire regimes, *P. Natl. Acad. Sci.*, 110, 6442–6447, doi:10.1073/pnas.1211466110, 2013.
- Arnell, A., Sitch, S., Pongratz, J., Stocker, B. D., Ciais, P., Poulter, B., Bayer, A. D., Bondeau, A., Calle, L., Chini, L. P., Gasser, T., Fader, M., Friedlingstein, P., Kato, E., Li, W., Lindeskog, M., Nabel, J. E. M. S., Pugh, T. A. M., Robertson, E., Viovy, N., Yue, C., and Zaehle, S.: Historical carbon dioxide emissions caused by land-use changes are possibly larger
10 than assumed, *Nat. Geosci.*, 10, 79–84, <https://doi.org/10.1038/ngeo2882>, 2017.
- Avitabile, V., Herold, M., Heuvelink, G. B. M., Lewis, S. L., Phillips, O. L., Asner, G. P., Armston, J., Ashton, P. S., Banin, L., Bayol, N., Berry, N. J., Boeckx, P., de Jong, B. H. J., DeVries, B., Girardin, C. A. J., Kearsley, E., Lindsell, J. A., Lopez-Gonzalez, G., Lucas, R., Malhi, Y., Morel, A., Mitchard, E. T. A., Nagy, L., Qie, L., Quinones, M. J., Ryan, C. M., Ferry, S. J. W., Sunderland, T., Laurin, G. V., Gatti, R. C., Valentini, R., Verbeeck, H., Wijaya, A. and Willcock, S.: An
15 integrated pan-tropical biomass map using multiple reference datasets, *Glob Change Biol*, 22: 1406–1420. doi:10.1111/gcb.13139, 2016.
- Bagley, J., A. Desai, K. Harding, P. Snyder & J. Foley: Drought and Deforestation: Has Land Cover Change Influenced Recent Precipitation Extremes in the Amazon? *Journal of Climate*, 27, 345-361, 2014.
- Best, M., Pryor, M., Clark, D., Rooney, G., Essery, R., Menard, C., Edwards, J., Hendry, M., Porson, A., Gedney, N., Mercado, L., Sitch, S., Blyth, E., Boucher, O., Cox, P., Grimmond, C., & Harding, R.: The Joint UK Land Environment Simulator (JULES), model description - Part 1: Energy and water fluxes, *Geoscientific Model Development*, 4, 677-699, 2011.
- 20 Betts, R.: Integrated approaches to climate-crop modelling: needs and challenges, *Philosophical Transactions of the Royal Society B-Biological Sciences*, 360, 2049-2065, 2005.
- Brando, P., J. Balch, D. Nepstad, D. Morton, F. Putz, M. Coe, D. Silverio, M. Macedo, E. Davidson, C. Nobrega, A. Alencar
25 & B. Soares: Abrupt increases in Amazonian tree mortality due to drought-fire interactions, *Proceedings of the National Academy of Sciences of the United States of America*, 111, 6347-6352, 2014.
- Burton, C., Betts, R.A., Jones, C.D., Williams, K.: Will fire danger be reduced by using Solar Radiation Management to limit global warming to 1.5 C compared to 2.0 C? *Geophysical Research Letters*. Apr 28;45(8):3644-52, 2018.
- Cano-Crespo, A., Oliveira, P., Boit, A., Cardoso, M., & Thonicke, K.: Forest edge burning in the Brazilian Amazon promoted
30 by escaping fires from managed pastures, *Journal of Geophysical Research-Biogeosciences*, 120, 2095-2107, 2015.
- Cardoso, M., Hurtt, G., Moore, B., Nobrem C., & Prins, E.: Projecting future fire activity in Amazonia, *Global Change Biology*, 9, 656-669, 2003.
- Cardoso, M., Nobre, C., Lapola, D., Oyama, M., Sampaio, G.: Long-term potential for fires in estimates of the occurrence of savannas in the tropics, *Global Ecology and Biogeography*, 17, 222–235. DOI: 10.1111/j.1466-8238.2007.00356.x, 2008.



- Castello, L. & Macedo, M.N.: Large-scale degradation of Amazonian freshwater ecosystems, *Global Change Biology*, 22, 990-1007, 2016.
- Ciais, P., Sabine, C., Bala, G., Bopp, L., Brovkin, V., Canadell, J., Chhabra, A., DeFries, R., Galloway, J., Heimann, M., Jones, C., Le Quéré, C., Myneni, R.B., Piao, S., and Thornton, P.: Carbon and Other Biogeochemical Cycles. In: *Climate Change 2013: The Physical Science Basis. Contribution of Working Group I to the Fifth Assessment Report of the Intergovernmental Panel on Climate Change* [Stocker, T.F., D. Qin, G.-K. Plattner, M. Tignor, S.K. Allen, J. Boschung, A. Nauels, Y. Xia, V. Bex and P.M. Midgley (eds.)]. Cambridge University Press, Cambridge, United Kingdom and New York, NY, USA, 2013.
- Clark, D., Mercado, L., Sitch, S., Jones, C., Gedney, N., Best, M., Pryor, M., Rooney, G., Essery, R., Blyth, E., Boucher, O., Harding, R., Huntingford C., & Cox, P.: The Joint UK Land Environment Simulator (JULES), model description - Part 2: Carbon fluxes and vegetation dynamics, *Geoscientific Model Development*, 4, 701-722, 2011.
- Cochrane, M. & Laurance, W.: Synergisms among Fire, Land Use, and Climate Change in the Amazon, *Ambio*, 37, 522-527, 2008.
- Coe, M., Marthews, T., Costa, M., Galbraith, D., Greenglass, N., Imbuzeiro, H., Levine, N., Malhi, Y., Moorcroft, P., Muza, M., Powell, T., Saleska, S., Solorzano, L., & Wang, J.: Deforestation and climate feedbacks threaten the ecological integrity of south-southeastern Amazonia, *Philosophical Transactions of the Royal Society B-Biological Sciences*, 368, 2013.
- Cox, P., Betts, R., Jones, C., Spall, S., & Totterdell, I.: Acceleration of global warming due to carbon-cycle feedbacks in a coupled climate model, *Nature*, 408, 184-187, 2000.
- Cox, P.M.: Description of the “TRIFFID” Dynamic Global Vegetation Model, Tech. Note 24, Hadley Centre, Met Office, 16 pp. 2001.
- ESA CCI <https://www.esa-landcover-cci.org/?q=node/175>, 2010.
- Cruzten, P.J., Heidt, L.E., Krasnec, J.P., Pollock, W.H., Seiler, W.G.: Biomass burning as a source of atmospheric gases CO, H₂, N₂O, NO, CH₃ Cl and COS, *Nature*, 282, 253, 1979.
- Flato, G., Marotzke, J., Abiodun, B., Braconnot, P., Chou, S.C., Collins, W., Cox, P., Driouech, F., Emori, S., Eyring, V., Forest, C., Gleckler, P., Guilyardi, E., Jakob, C., Kattsov, V., Reason, C., and Rummukainen, M.: Evaluation of Climate Models. In: *Climate Change 2013: The Physical Science Basis. Contribution of Working Group I to the Fifth Assessment Report of the Intergovernmental Panel on Climate Change* [Stocker, T.F., D. Qin, G.-K. Plattner, M. Tignor, S.K. Allen, J. Boschung, A. Nauels, Y. Xia, V. Bex and P.M. Midgley (eds.)]. Cambridge University Press, Cambridge, United Kingdom and New York, NY, USA, 2013.
- Giglio, L., Randerson, J. T., and Werf, G. R.: Analysis of daily, monthly, and annual burned area using the fourth generation global fire emissions database (GFED4), *J. Geophys. Res.- Biogeo.*, 118, 317-328, 2013.
- Good, P., Lowe, J., Ridley, J., Bamber, J., Payne, T., Keen, A., Stroeve, J., Jackson, L., Srokosz, M., Kay, G., Harper, A., Kruijt, B., Burke, E., Abbott, B., O’Connor, F., Minshull, T., Turley, C., Williamson, P.: Post-AR5 literature review on large-scale systems with potential for abrupt and/or irreversible change. AVOID publication report, 2014.



- Hantson, S., Arneth, A., Harrison, S., Kelley, D., Prentice, I., Rabin, S., Archibald, S., Mouillot, F., Arnold, S., Artaxo, P., Bachelet, D., Ciais, P., Forrest, M., Friedlingstein, P., Hickler, T., Kaplan, J., Kloster, S., Knorr, W., Lasslop, G., Li, F., Mangeon, S., Melton, J., Meyn, A., Sitch, S., Spessa, A., van der Werf, G., Voulgarakis, A., & Yue, C.: The status and challenge of global fire modelling, *Biogeosciences*, 13, 3359–3375, 2016.
- 5 Harper, A., Cox, P., Friedlingstein, P., Wiltshire, A., Jones, C., Sitch, S., Mercado, L., Groenendijk, M., Robertson, E., Kattge, J., Bonisch, G., Atkin, O., Bahn, M., Cornelissen, J., Niinemets, U., Onipchenko, V., Penuelas, J., Poorter, L., Reich, P., Soudzilovskaia, N., & van Bodegom, P.: Improved representation of plant functional types and physiology in the Joint UK Land Environment Simulator (JULES v4.2) using plant trait information, *Geoscientific Model Development*, 9, 2415–2440, 2016.
- 10 Harper, A. B., Wiltshire, A. J., Cox, P. M., Friedlingstein, P., Jones, C. D., Mercado, L. M., Sitch, S., Williams, K., and Duran-Rojas, C.: Vegetation distribution and terrestrial carbon cycle in a carbon-cycle configuration of JULES4.6 with new plant functional types, *Geosci. Model Dev. Discuss.*, <https://doi.org/10.5194/gmd-2017-311>, in review, 2018.
- Hartley, A., MacBean, N., Georgievski, G., Bontemps, S.: Uncertainty in plant functional type distributions and its impact on land surface models. *Remote Sensing of Environment*, ISSN 0034-4257, <https://doi.org/10.1016/j.rse.2017.07.03>, 2017.
- 15 Hurtt, G.C., Frohling, S., Fearon, M.G., Moore, B., Shevliakova, E., Malyshev, S., Pacala, S.W., Houghton, R.A.: The underpinnings of land-use history: three centuries of global gridded land-use transitions, wood harvest activity, and resulting secondary lands, *Global Change Biol* 12:1208–1229, 2006.
- Hurtt, G., Chini, L., Frohling, S., Betts, R., Feddema, J., Fischer, G., Fisk, J., Hibbard, K., Houghton, R., Janetos, A., Jones, C., Kindermann, G., Kinoshita, T., Goldewijk, K., Riahi, K., Shevliakova, E., Smith, S., Stehfest, E., Thomson, A.,
20 Thornton, P., van Vuuren, D., & Wang, Y.: Harmonization of land-use scenarios for the period 1500–2100: 600 years of global gridded annual land-use transitions, wood harvest, and resulting secondary lands, *Climatic Change*, 109, 117–161, 2011.
- Jones, C., Hughes, J., Bellouin, N., Hardiman, S., Jones, G., Knight, J., Liddicoat, S., O'Connor, F., Andres, R., Bell, C., Boo, K., Bozzo, A., Butchart, N., Cadule, P., Corbin, K., Doutriaux-Boucher, M., Friedlingstein, P., Gornall, J., Gray, L.,
25 Halloran, P., Hurtt, G., Ingram, W., Lamarque, J., Law, R., Meinshausen, M., Osprey, S., Palin, E., Chini, L., Raddatz, T., Sanderson, M., Sellar, A., Schurer, A., Valdes, P., Wood, N., Woodward, S., Yoshioka, M., & Zerroukat, M.: The HadGEM2-ES implementation of CMIP5 centennial simulations, *Geoscientific Model Development*, 4, 543–570, 2011.
- Kelley, D. I., Prentice, I. C., Harrison, S. P., Wang, H., Simard, M., Fisher, J. B., and Willis, K. O.: A comprehensive benchmarking system for evaluating global vegetation models, *Biogeosciences*, 10, 3313–3340, doi: 10.5194/bg-10-3313-
30 2013, 2013.
- Kelley, D. I., Sandy P. Harrison, and I. C. Prentice.: Improved simulation of fire–vegetation interactions in the Land surface Processes and eXchanges dynamic global vegetation model (LPX-Mv1), *Geoscientific Model Development* 7.5: 2411–2433, 2014.



- Kloster, S., and Lasslop, G.: Historical and future fire occurrence (1850 to 2100) simulated in CMIP5 Earth System Models, *Global and Planetary Change* 150 (2017): 58-69, 2017.
- Lasslop, G., Kirsten T., and Kloster, S.: SPITFIRE within the MPI Earth system model: Model development and evaluation, *Journal of Advances in Modeling Earth Systems* 6.3: 740-755, 2014.
- 5 Lasslop, G., Brovkin, V., Reick, C.H., Bathiany, S., Kloster, S.: Multiple stable states of tree cover in a global land surface model due to a fire-vegetation feedback, *Geophysical Research Letters*. Jun 28;43(12):6324-31, 2016.
- Laurance, W. F., Vasconcelos, H. L., Lovejoy, T. E.: Forest loss and fragmentation in the Amazon: implications for wildlife conservation, *Oryx* 34:39 – 45.DOI: 10.1046/j.1365-3008.2000.00094.x, 2000.
- Le Quéré, C., Andrew, R. M., Canadell, J. G., Sitch, S., Korsbakken, J. I., Peters, G. P., Manning, A. C., Boden, T. A., Tans,
10 P. P., Houghton, R. A., Keeling, R. F., Alin, S., Andrews, O. D., Anthoni, P., Barbero, L., Bopp, L., Chevallier, F., Chini, L. P., Ciais, P., Currie, K., Delire, C., Doney, S. C., Friedlingstein, P., Gkritzalis, T., Harris, I., Hauck, J., Haverd, V., Hoppema, M., Klein Goldewijk, K., Jain, A. K., Kato, E., Körtzinger, A., Landschützer, P., Lefèvre, N., Lenton, A., Lienert, S., Lombardozzi, D., Melton, J. R., Metzl, N., Millero, F., Monteiro, P. M. S., Munro, D. R., Nabel, J. E. M. S., Nakaoka, S.-I., O'Brien, K., Olsen, A., Omar, A. M., Ono, T., Pierrot, D., Poulter, B., Rödenbeck, C., Salisbury, J., Schuster, U.,
15 Schwinger, J., Séférian, R., Skjelvan, I., Stocker, B. D., Sutton, A. J., Takahashi, T., Tian, H., Tilbrook, B., van der Laan-Luijkx, I. T., van der Werf, G. R., Viovy, N., Walker, A. P., Wiltshire, A. J., and Zaehle, S.: Global Carbon Budget 2016, *Earth Syst. Sci. Data*, 8, 605-649, <https://doi.org/10.5194/essd-8-605-2016>, 2016.
- Li, F., Zeng, X., & Levis, S.: A process-based fire parameterization of intermediate complexity in a Dynamic Global Vegetation Model, *Biogeosciences*, 9, 2761-2780, 2012.
- 20 López-Saldaña, G., Bistinas, I., Pereira, J.M.: Global analysis of radiative forcing from fire-induced shortwave albedo change, *Biogeosciences*, 2015.
- Mangeon, S., Voulgarakis, A., Gilham, R., Harper, A., Sitch, S., & Folberth, G.: INFERNO: a fire and emissions scheme for the UK Met Office's Unified Model, *Geoscientific Model Development*, 9, 2016.
- Pellegrini, A. F. A., Anderegg, W. R. L., Paine, C. E. T., Hoffmann, W. A., Kartzinel, T., Rabin, S. S., Sheil, D., Franco, A.
25 C. and Pacala, S. W.: Convergence of bark investment according to fire and climate structures ecosystem vulnerability to future change, *Ecol Lett*, 20: 307–316. doi:10.1111/ele.12725, 2017.
- Poulter, B., MacBean, N., Hartley, A., Khlystova, I., Arino, O., Betts, R., Bontemps, S., Boettcher, M., Brockmann, C., Defourny, P., Hagemann, S., Herold, M., Kirches, G., Lamarche, C., Lederer, D., Ottlé, C., Peters, M., and Peylin, P.: Plant
30 functional type classification for earth system models: results from the European Space Agency's Land Cover Climate Change Initiative, *Geosci. Model Dev.*, 8, 2315-2328, <https://doi.org/10.5194/gmd-8-2315-2015>, 2015.
- Prentice, I. C., et al.: Modeling fire and the terrestrial carbon balance, *Global Biogeochemical Cycles* 25.3, 2011.
- Rabin, S. S., S. L. Malyshev, B. I. Magi, E. Shevliakova & S. W. Pacala: A fire model with distinct crop, pasture, and non-agricultural burning: Use of new data and a model-fitting algorithm for FINALv1, *Geosci. Model Dev. Discuss.*, 2017, 1-48, 2017a.



- Rabin, S. S., Melton, J. R., Lasslop, G., Bachelet, D., Forrest, M., Hantson, S. et al: The Fire Modeling Intercomparison Project (FireMIP), phase 1: experimental and analytical protocols with detailed model descriptions, *Geoscientific Model Development*, 10(3), 1175-1197, 2017b.
- 5 Randerson, J., Chen, Y., van der Werf, G., Rogers, B., and Morton, D.: Global burned area and biomass burning emissions from small fires, *Journal of Geophysical Research*, 117, G04012, doi:10.1029/2012JG002128, 2012.
- Settele, J., R. Scholes, R. Betts, S. Bunn, P. Leadley, D. Nepstad, J.T. Overpeck, and M.A. Taboada: Terrestrial and inland water systems. In: *Climate Change 2014: Impacts, Adaptation, and Vulnerability. Part A: Global and Sectoral Aspects. Contribution of Working Group II to the Fifth Assessment Report of the Intergovernmental Panel on Climate Change* [Field, C.B., V.R. Barros, D.J. Dokken, K.J. Mach, M.D. Mastrandrea, T.E. Bilir, M. hatterjee, K.L. Ebi, Y.O. Estrada, 10 R.C. Genova, B. Girma, E.S. Kissel, A.N. Levy, S. MacCracken, P.R. Mastrandrea, and L.L. White (eds.)]. Cambridge University Press, Cambridge, United Kingdom and New York, NY, USA, pp. 271-359, 2014.
- Shakesby, R.A., Doerr, S.H.: Wildfire as a hydrological and geomorphological agent, *Earth-Science Reviews*. Feb 1;74(3-4):269-307, 2006.
- 15 Sitch, S., Friedlingstein, P., Gruber, N., Jones, S., Murray-Tortarolo, G., Ahlstrom, A., Doney, S., Graven, H., Heinze, C., Huntingford, C., Levis, S., Levy, P., Lomas, M., Poulter, B., Viovy, N., Zaehle, S., Zeng, N., Arneth, A., Bonan, G., Bopp, L., Canadell, J., Chevallier, F., Ciais, P., Ellis, R., Gloor, M., Peylin, P., Piao, S., Le Quéré, C., Smith, B., Zhu Z., & Myneni, R.: Recent trends and drivers of regional sources and sinks of carbon dioxide, *Biogeosciences*, 12, 653-679, 2015.
- Soares-Filho, B., Nepstad, D., Curran, L., Cerqueira, G., Garcia, R., Ramos, C., Voll, E., McDonald, A., Lefebvre, P., Schlesinger, P.: Modelling conservation in the Amazon basin, *Nature Letters*, Vol 440, doi 101038/nature04389, 2006.
- 20 Staver, A. C., Archibald, S., and Levin, S. A.: The global extent and determinants of savanna and forest as alternative biome states, *Science*, 334, 230–232, doi:10.1126/science.1210465, 2011.
- van der Werf, G. R. et al.: Global fire emissions estimates during 1997–2016. *Earth System Science Data* 9, 697–720, 2017.
- Watson, R.T., Noble, I.R., Bolin, B., Ravindranath, N.H., Verardo, D.J., and Dokkenm D.J. (Eds.) IPCC
Cambridge University Press, UK. pp 375. Available from Cambridge University Press, The Edinburgh Building
25 Shaftesbury Road, Cambridge CB2 2RU ENGLAND, 2000.